https://doi.org/10.5194/egusphere-2026-2262
Preprint. Discussion started: 26 May 2026

BlueMinerva: An integrated, autonomous platform for carbon flux and environmental monitoring at the aquatic–atmospheric interface in low-flow waterbodies

Judith Vogt[1], Tarek S. El-Madany[1], Christian Burgold[1], Abdullah Bolek[1], Elliot Pratt[1], Torsten Sachs[2,3], Christian Wille[2], Manuel Helbig[2,4], Maximilian P. Lau[5,6], Sebastian Zug[7], Jörg Matschullat[5,8], and Mathias Göckede[1]

[1]Max Planck Institute for Biogeochemistry, Jena, Germany
[2]GFZ Helmholtz Centre for Geosciences, Potsdam, Germany
[3]Institute of Geoecology, Technische Universität Braunschweig, Braunschweig, Germany
[4]Department of Physics and Atmospheric Sciences, Dalhousie University, Halifax, NS, Canada
[5]Interdisciplinary Environmental Research Centre, TU Bergakademie Freiberg, Freiberg, Germany
[6]Institute of Mineralogy, TU Bergakademie Freiberg, Freiberg, Germany
[7]Institute of Computer Science, TU Bergakademie Freiberg, Freiberg, Germany
[8]Arthur L. Irving Institute, Dartmouth College, Hanover, NH, USA

Correspondence: Judith Vogt (jvogt@bgc-jena.mpg.de)

Abstract.

Water-air fluxes of carbon dioxide (CO_2) and methane (CH_4) in lakes exhibit substantial spatial heterogeneity, often varying across remarkably fine spatial scales. While manual flux chamber measurements offer high spatial resolution and the potential to capture this variability, their application is typically constrained by labor intensity and logistical limitations. In contrast, eddy covariance (EC) measurements integrate fluxes over a larger footprint, effectively averaging over spatial gradients and complicating a process-based interpretation of the data. Bridging this gap requires methods that combine spatial precision with scalable, continuous monitoring – essential for advancing our mechanistic understanding of lake carbon dynamics.

To facilitate highly resolved biogeochemical measurements, we developed BlueMinerva, an autonomous platform to monitor surface carbon fluxes with the static chamber method, and simultaneously determine physicochemical, biological, bathymetric, and meteorological variables at pre-defined locations. The platform can be programmed to navigate a user-defined track across a waterbody, and collect flux and ancillary data both in transit and at fixed locations for several hours to days, depending on the sensor configuration and related battery requirements.

We deployed the setup at Dagow Lake (Germany) and in a small lake in the Stordalen Mire (Sweden). In total, we obtained 485 chamber-derived flux estimates over 72 measurement hours. We compared CO_2 flux estimates between measurements with two different gas analyzers that were simultaneously mounted on the BlueMinerva. The lower-cost sensor (CARBOCAP GMP343, Vaisala) performed equally well as the precise, but costlier sensor (LI-7810, LI-COR) as long as measurements were sufficiently long (around 5 min). Furthermore, we compared measured carbon fluxes with those from an eddy covariance tower at Dagow Lake where CH_4 fluxes diverged slightly, possibly linked to the usage of different sensors (closed-path versus open-path), while magnitudes of CO_2 fluxes matched well. At both lakes, we identified areas of higher emissions, especially for

https://doi.org/10.5194/egusphere-2026-2262
Preprint. Discussion started: 26 May 2026

CH_4, and were thus able to resolve the spatial variability of carbon fluxes within the waterbodies. Concurrently, we measured differences in meteorological conditions, and critical limnological variables (water temperature, specific conductivity, pH, dissolved oxygen, chlorophyll, phycocyanin, turbidity, and fluorescent dissolved organic matter) – valuable measurements that enable a comprehensive assessment of environmental drivers behind flux variability.

We conclude that platforms like the BlueMinerva have the potential to be adopted widely by scientists and stakeholders to better capture biogeochemical processes in lakes at high spatial and temporal resolution.

1 Introduction

The amount of carbon exchanged between the water surface and the atmosphere often shows pronounced spatial variation within lakes (Natchimuthu et al., 2016, 2017; Loken et al., 2019; Sø et al., 2023). Spatial variability in flux rates can be introduced, for example, by gradients in bathymetry (Spafford and Risk, 2018; Yin et al., 2025), coverage by vegetation with different community structure (Desrosiers et al., 2022), or lateral influx of groundwater discharge (Tian et al., 2025). The resulting variability in carbon cycle processes makes it difficult to estimate net lake flux budgets based on a small number of sampling points obtained at fine scales. Meanwhile, integrated signals from observations at a coarser resolution are difficult to interpret because they combine multiple carbon sources and sinks. To capture this spatial variability using in situ flux measurements, an extensive, spatially resolved survey of the lake surface is therefore required.

For long-term monitoring, the eddy covariance method can be used to determine ecosystem-scale carbon fluxes. However, the associated footprint extent and coverage vary over time due to changes in atmospheric stability, wind speed and direction. Consequently, the footprint may not cover the entire lake and may, for example, overlook littoral areas with potentially higher fluxes (Juutinen et al., 2003; Spafford and Risk, 2018). Moreover, particularly for smaller lakes the footprint regularly reaches beyond the shoreline, therefore mixing the lake flux signals with those from the surrounding terrain. While the eddy covariance method can yield a high temporal resolution under favorable conditions, spatial gradients of carbon fluxes within waterbodies remain unresolved. In addition, the quantification of comparatively low flux rates from the water surface may be affected by the inclusion of terrestrial signals, which can differ substantially from those of the waterbody.

Flux measurements conducted at smaller scales are thus better suited to obtain a good understanding of spatial differences in flux signals across the lake surface. Manually operated floating chambers provide a low-cost, simple measurement technique that is suitable for water-air carbon flux measurements, although restricted to manual labor and episodic sampling events (Kremer et al., 2003). To better capture temporal dynamics in aquatic carbon fluxes, in recent years automatic flux chambers were developed and deployed on lakes (Than Duc et al., 2013; Martinsen et al., 2018; Spafford and Risk, 2018; Gerardo-Nieto et al., 2019; Dietrich et al., 2025). This technique facilitates the collection of continuous flux measurements, albeit only at fixed locations. Spatially explicit automated platforms for biogeochemical and hydrological measurements beneath the water surface evolved simultaneously (Crawford et al., 2015). Truly autonomous high-tech platforms including CO_2 flux measurements for waterbodies only emerged recently (Pose et al., 2023; Zug et al., 2025); however, the development and application of such systems still requires extensive knowledge about robotics. In addition, autonomous platforms for CH_4 fluxes

https://doi.org/10.5194/egusphere-2026-2262
Preprint. Discussion started: 26 May 2026

were developed previously, but detection limits of integrated analyzers restrict measurements at low-emitting waterbodies (Dunbabin and Grinham, 2017).

To provide an easy-to-use and flexible mobile observational system, we developed BlueMinerva, a simplified autonomous platform for water surface measurements of CO_2 and CH_4 fluxes, physicochemical and biological indicators, and bathymetry, accompanied by a suite of meteorological measurements (Fig. 1). Here, we provide an overview on the technical setup and capabilities, followed by an assessment of system performance under various conditions and a discussion of the limitations of and the opportunities arising with the BlueMinerva. First, we assessed the agreement between a silicon-based non-dispersive infrared CO_2 analyzer (CARBOCAP GMP343, Vaisala) and a precise optical-feedback cavity-enhanced absorption spectroscopic analyzer of CO_2 and CH_4 (LI-7810, LI-COR) which can simultaneously be deployed on the platform. In addition, we compared the measured spatially resolved fluxes with those from a reference eddy covariance tower. Finally, we show results on the spatial heterogeneity in aquatic carbon fluxes and ancillary measurements at two test sites, a temperate lake in northeastern Germany, and a sub-Arctic lake in northern Sweden.

Figure 1. A picture of the BlueMinerva on a lake at Stordalen Mire.

https://doi.org/10.5194/egusphere-2026-2262
Preprint. Discussion started: 26 May 2026

2 Materials and Methods

2.1 Test sites

The BlueMinerva was tested at Dagow Lake (Latitude: 53.1514°N, Longitude: 13.0543°E) in northeastern Germany and at Inre Harrsjön (Latitude: 68.3584°N, Longitude: 19.0460°E) in the Stordalen Mire in northern Sweden (Fig. 2).

Dagow Lake is a mesotrophic waterbody with a mean depth of around 5 m, a maximum depth of approximately 9 m and a surface area of 0.24 km^2 (Casper et al., 2009; Guseva et al., 2023). The glacial lake is surrounded by beech forest. Measurements at Dagow Lake were conducted on May 13-16, 2025, and covered both daytime and nighttime periods. The air temperatures ranged between 7 and 20°C, westerly winds prevailed, and marginal rain occurred in the afternoon of May 15. These and more measurements were obtained from an eddy covariance tower situated in the center of the lake where CO_2 fluxes were measured with the Enclosed CO_2/H_2O Analyzer LI-7200 (LI-COR, USA), and CH_4 fluxes with the Open Path CH_4 Analyzer LI-7700 (LI-COR, USA) at 1.97 m above the water surface.

For the deployment at a high-latitude lake, we tested the BlueMinerva at Inre Harrsjön, a small lake with a maximum depth of 5.4 m and a surface area of 0.02 km^2 (Wik et al., 2013). The lake is part of a network of multiple lakes within the Stordalen Mire complex that are connected by narrow and shallow channels, while the outlet of Inre Harrsjön is located at the northwestern end. The lake is mostly surrounded by wet fens, and a few degrading palsas. Measurements at Inre Harrsjön were conducted in daylight on July 9, 10, 13 and 16, 2025. During this time, air temperatures ranged between 5 and 23°C and no rain was observed according to hourly data from the Swedish Meteorological and Hydrological Institute for the Abisko Automatic Station (Latitude: 68.3538°N, Longitude: 18.8164°E) (Swedish Meteorological and Hydrological Institute (SMHI), 2025).

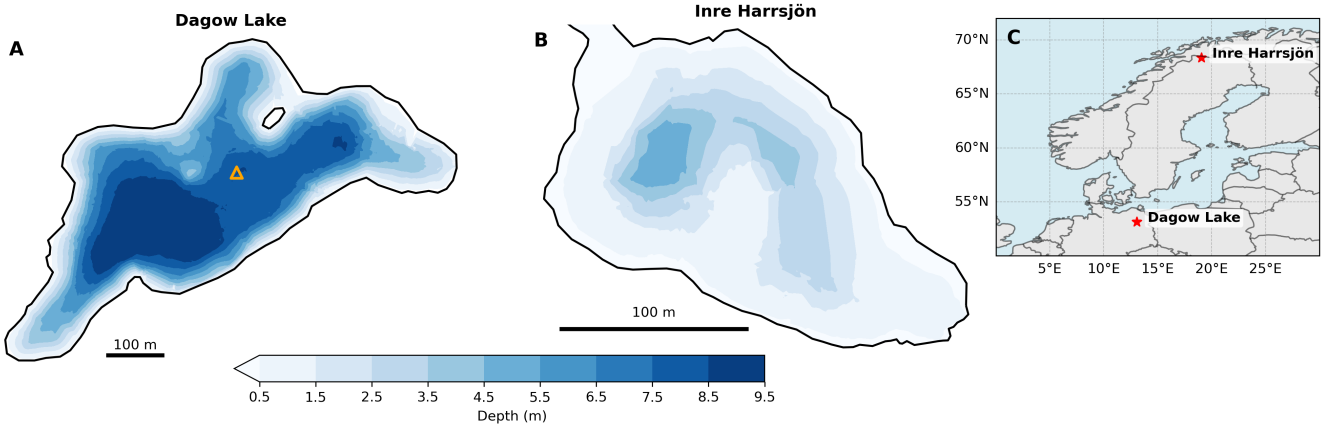

Figure 2. The test sites Dagow Lake in northeastern Germany (panel A) and Inre Harrsjön in the Stordalen Mire in northern Sweden (B). The contours indicate lake bathymetry based on measured and interpolated water depths. The orange triangle marks the location of the eddy covariance tower at Dagow Lake. The locator map (C) shows the test sites in northern Europe, with basemap data provided by Natural Earth (https://naturalearthdata.com) accessed via Cartopy.

https://doi.org/10.5194/egusphere-2026-2262
Preprint. Discussion started: 26 May 2026

2.2 Instrumental setup

The BlueMinerva is composed of off-the-shelf components listed in Table 1 and shown in Fig. 3. The BlueBoat Uncrewed Surface Vessel (BlueRobotics, USA) serves as a propeller-driven platform for chamber flux, water quality, meteorological and bathymetric measurements. To conduct chamber flux measurements, we installed an opaque chamber, 25 cm in height and diameter. The lowering and lifting of the chamber is facilitated by pneumatic pistons driven by a vacuum pump (NMP 850, Diaphragm Gas Pump, KNF Neuberger GmbH, Germany). As the chamber is lowered, approximately 6 cm of the bottom of the chamber is submerged, to guarantee a tight seal of the chamber headspace during measurements. The chamber is connected in a closed loop with two greenhouse gas analyzers: a portable analyzer with Optical Feedback–Cavity Enhanced Absorption Spectroscopy (LI-7810, LI-COR, USA; hereafter: LI-7810) measuring wet and dry mole fractions of CO_2 and CH_4 every second, and a silicon-based non-dispersive infrared sensor (CARBOCAP Carbon Dioxide Probe GMP343, Vaisala, Finland; hereafter: GMP343) collecting wet CO_2 mole fractions at 0.5 Hz.

The CO_2 analyzer GMP343 (approximately 4,000 EUR) has been used widely for aquatic chamber flux measurements given its comparatively low cost and high performance (Oviedo-Vargas et al., 2016; Spafford and Risk, 2018; Dubey et al., 2024). We used the diffusion model of the analyzer with a custom-built enclosure for flow-through measurements. The LI-7810, the second analyzer used in this study, performs especially well measuring CH_4, but also comes with a substantially higher cost (approximately 40,000 EUR). For CO_2 measurements, the LI-7810 has a specified precision of 3.5 ppm at 400 ppm with 1 s averaging, whereas the GMP343 manufacturer specification implies an accuracy of 3 ppm plus 1% of the measured mole fractions. It should be noted that precision and accuracy metrics as specified in instrument datasheets cannot be directly compared; however, they both provide valuable context for understanding measurement performance, and indicate lower short-term measurement noise under stable conditions for the LI-7810. For CH_4 measurements, the LI-7810 has a precision of 0.6 ppb at 2 ppm with 1 s averaging, and offers substantially higher resolution of small changes in CH_4 mole fractions than sensors used in previous autonomous setups (Dunbabin and Grinham, 2017).

A fan circulates the air within the chamber, while air temperature, relative humidity (RH) and pressure are recorded both inside and outside the chamber and a GPS records the location of the platform. In addition, we deployed a 2D anemometer (LI-550 Trisonica Mini, LI-COR, USA) at approximately 1 m above the water surface to determine the wind speed.

For observations below the water surface, a multiparameter water quality sonde (EXO2, YSI, USA) is used to measure water temperature, pH, specific conductivity, dissolved oxygen (DO), fluorescent dissolved organic matter (fDOM), chlorophyll and phycocyanin concentrations approximately 10 cm below the water surface. Once an hour, the sensors of the sonde are automatically wiped with an integrated wiper. The water depth is measured with a single beam echosounder (Ping2, BlueRobotics, USA) that is mounted facing downward just below the water surface. In addition to scanning the water surface while the BlueMinerva is operating autonomously, the sonde can be lowered manually into the water column in order to conduct depth profiles.

https://doi.org/10.5194/egusphere-2026-2262
Preprint. Discussion started: 26 May 2026

All components of the measurement platform are powered by batteries and all data are logged at 1 Hz on a datalogger (CR1000X, Campbell Scientific, USA), which was fitted in a waterproof case (yellow box in Fig. 1). The dimensions of the BlueMinerva are 122.5 cm in height, 191 cm in length and 91 cm in width. The total weight amounts to 57 kg.

Table 1. Overview of the main components of the BlueMinerva and their function.

Component	Manufacturer	Function
BlueBoat	BlueRobotics, USA	Autonomous platform for instrumental setup
LI-7810	LI-COR, USA	CO_2 and CH_4 analyzer
CARBOCAP GMP343	Vaisala, Finland	CO_2 analyzer
GPS 16x-HVS	Garmin, USA	GPS
KPK-ME	Galltec+MELA, Germany	Ambient temperature and relative humidity sensor inside the chamber
CPC-ME	Galltec+MELA, Germany	Ambient temperature and relative humidity sensor outside the chamber
Barometric pressure sensor 61402V	R.M. Young, USA	Pressure sensor
LI-550 Trisonica Mini	LI-COR, USA	Measurements of wind speed
Ping2 Sonar	BlueRobotics, USA	Measurements of water depth
EXO2	YSI, USA	Multiparameter sonde for physico-chemical and biological subsurface measurements
CR1000X	Campbell Scientific, USA	Datalogger to record all data

2.3 Implementing measurement trajectories

The measurements were primarily conducted on missions lasting several hours at a time, following a user-defined path across the lake area both during the day and at night (Fig. A1). The missions were designed with the ground-control and mission-planning software Mission Planner (ArduPilot Dev Team, 2024) developed for unmanned aerial systems, and subsequently uploaded to the BlueBoat. A mission was started once the BlueMinerva was in the water, all instruments were turned on and warmed up. The measurement platform moved at a cruising speed of approximately 1 m/s during transit. Once arrived at a pre-defined measurement location, the platform was programmed to loiter, aiming at maintaining the position with minimum use of the propellers in order to minimize disturbance of the measurement conditions. This implies that the platform automatically maneuvered back to the original measurement location during a measurement if it drifted away due to wind or current. After a measurement had finished, the platform autonomously moved on to the next measurement location (Fig. A1).

https://doi.org/10.5194/egusphere-2026-2262
Preprint. Discussion started: 26 May 2026

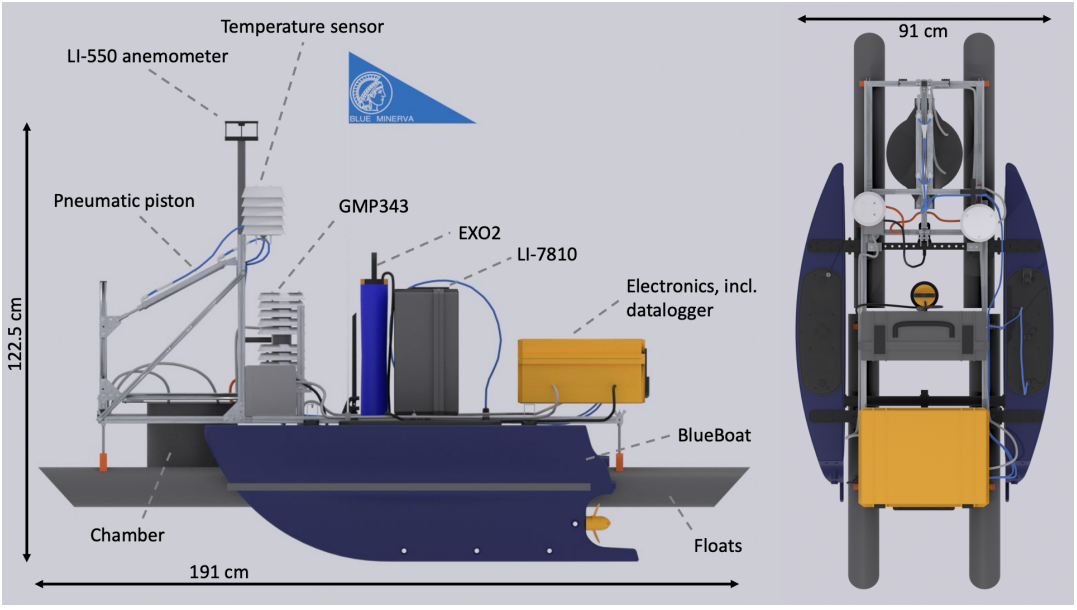

Figure 3. Technical drawing of the BlueMinerva from a side (left) and top view (right). The main components are listed in Table 1. The drawing was produced with the Blender software. Credit: István Héjja.

2.4 Platform performance

To quantify how well the platform maintained its position during individual measurements, we determined the centroid across the positions of the BlueMinerva and the median distance of individual positions to the centroid, which represents the Circular Error Probable (CEP). This measure indicates the radius within which 50% of the recorded positions fall.

To determine how severely the BlueMinerva formed waves on the water surface during chamber measurements, we determined the Froude number (Fr),

$$Fr = \frac{U}{\sqrt{gL}}, \tag{1}$$

with the platform speed U, the acceleration of gravity $g = 9.81$ m s^{-2}, and the length of the platform L. Subsequently, we quantified the Reynolds number (Re) to verify that viscous effects can be neglected in the propeller slipstream,

$$Re = \frac{U_{slip} D}{\nu}, \tag{2}$$

with the maximum water speed in the propeller's slipstream (U_{slip}), the propeller diameter ($D = 0.122$ m), and the kinematic viscosity of freshwater at 20°C ($\nu = 1.004 \cdot 10^{-6}$ m^2 s^{-1}), and using

$$U_{slip} = \frac{K_v \cdot V}{60} \pi D, \tag{3}$$

https://doi.org/10.5194/egusphere-2026-2262
Preprint. Discussion started: 26 May 2026

where $K_v = 470$ RPM V^{-1} is the motor velocity, and V represents a voltage of 16 V assuming fully charged batteries. Then, we used a turbulent jet model with the centerline velocity of the jet (U_{decay}) decaying as

$$U_{decay}(x) \approx U_{slip}(\frac{x}{D})^{-1}, \quad (4)$$

where $x = 0.95$ m denotes the distance between the propeller and the chamber.

2.5 Technical details

2.5.1 Communication features

The BlueBoat component enables autonomous navigation on a waterbody through pre-programmed trajectories, facilitated by a Navigator Flight Controller expansion board connected to the onboard Raspberry Pi 4, in combination with the ArduRover control firmware and wireless communication tools. An adequate mission-planning software, MissionPlanner in this case, aids in communicating the user-defined trajectory including loiter times to the BlueBoat. To time the chamber measurements so that they occurred when the platform was loitering and maintaining its position, we additionally implemented a communication scheme between the datalogger and the BlueBoat with a program based on the Campbell Scientific programming language CRBasic.

By default, all environmental data (meteorological, bathymetric, and physicochemical and biological variables) were saved at 1 Hz on the datalogger, whether the platform was in transit or loitering at a user-defined sampling spot. During transit, the chamber was open, and no signals from the gas analyzers were stored. Once the platform reached a measurement location, the BlueBoat was programmed to turn on a 5 V output signal of the Raspberry Pi for two seconds when it reached a measurement location. This 5 V signal was detected by the CR1000X datalogger to initiate the measurement sequence of the chamber.

At this point, the measurement cycle began following the communication scheme (Fig. 4). First, the fan inside the chamber turned on to circulate the air within the chamber to prevent any potential changes in mole fractions absorbed during transit. Simultaneously, an external pump (Schwarzer SPS 622) was turned on by the CR1000X to flush the air inside the tubes and the measurement cell of the GMP343 with ambient air from inside the chamber. The LI-7810 was continuously flushed by its internal pump. Both gas analyzers were connected in independent closed loops with the chamber to account for different flow rates of the respective pumps. The venting time was pre-defined at 45 s before and after the measurements. This time also allowed for the system to equilibrate as the platform stopped transiting and the propellers only turned on as needed to maintain the location. Subsequently, the chamber was lowered by pneumatic pistons. This process initiated the gas exchange between the water surface and the sealed chamber headspace as well as the collection of chamber data (gas mole fractions, temperature and humidity). After the pre-defined duration of the measurement (e.g. 300 s), the chamber data collection stopped and the chamber opened using the pneumatic pistons. Another ventilation period began in order to flush the unit and prevent gas from being carried over to the next measurement. Following the transit to the next user-defined position, this cycle started again once the next measurement location was reached and the 5-V signal was sent out anew.

Another operating mode of the BlueMinerva is the static mode, where the location is either program-controlled (e.g. by using the unlimited loitering mode in MissionPlanner) or mechanically maintained by anchoring or tying the platform, or where the

https://doi.org/10.5194/egusphere-2026-2262
Preprint. Discussion started: 26 May 2026

platform is free-floating without the propellers turned on. In this case, the measurement cycle functioned as outlined in Fig. 4, except that no signal was received, but rather the measurement cycle was repeated in a loop based on the pre-defined ventilation and measurement times.

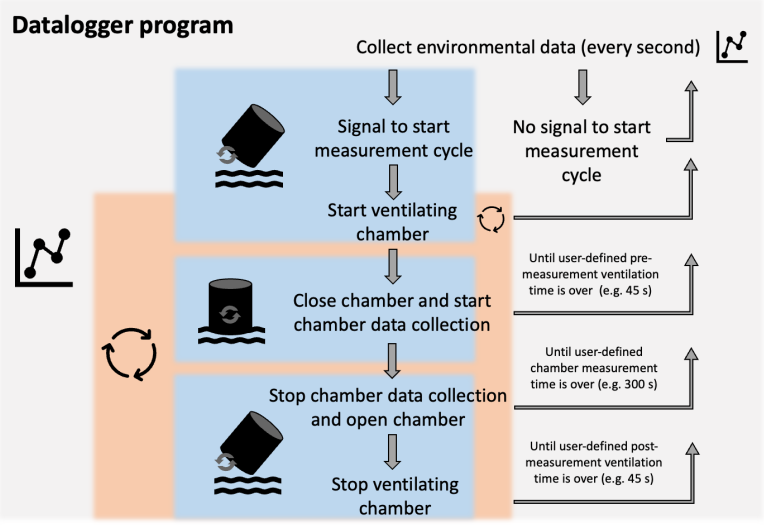

Figure 4. An overview of the communication scheme embedded in the datalogger program.

2.5.2 Power supply

The BlueMinerva was powered by several batteries (Table 2). The stated quantities were needed to operate the platform at any given time. However, additional batteries are recommended to allow swapping and thereby minimize interruptions to operation. In our setup, we kept an additional set of the three times two batteries for exchange, which allowed for almost continuous measurements, provided that batteries were manually exchanged as needed. The operational time was mainly limited by the batteries of the LI-7810 gas analyzer, which required replacement every 6–8 hours. If the measurement time of the analyzer were to be extended (e.g. by installing additional external batteries, or solar panels), also more batteries would be needed to power the remaining components. While adding batteries or solar panels can extend the operational time of the BlueMinerva, this comes with a trade-off between increased data acquisition and added payload, which could theoretically be overcome with attaching additional floats.

2.5.3 Performance features

At Dagow Lake, the BlueMinerva showed a maximum CEP of 0.77 m, and at Inre Harrsjön a maximum CEP of 1.00 m. The GPS-derived speed of the BlueMinerva ranged between 0–0.72 m s^{-1} during measurements, and up to 1.65 m s^{-1} during

https://doi.org/10.5194/egusphere-2026-2262
Preprint. Discussion started: 26 May 2026

Table 2. List of all six batteries needed to power and run the BlueMinerva with all components listed in Table 1. RH refers to relative humidity.

Type	Manufacturer	Nominal voltage (V)	Capacity (Ah)	Weight (kg)	Consumer	Quantity
Lithium-ion battery (18650 cells, 4S6P)	BlueRobotics, USA	14.8	18	1.18	BlueBoat	2
Lithium-ion battery (P/N 442-11807)	Inspired Energy, USA	14.4	6.8	0.45	LI-7810	2
Lithium Iron Phosphate Battery (LiFePO4) CUBE	Green Cell, Poland	12.8	10	1.00	GMP343, GPS, 2x Temp/RH, Pressure sensor, LI-550, Ping2, EXO2, CR1000X, pumps	2

transit at Dagow Lake. At Inre Harrsjön, the speed during measurements ranged from 0–0.41 m s^{-1} and reached 1.13 m s^{-1} during transit. With the resulting maximum Froude number during measurements being 0.17 at Dagow Lake and 0.10 at Inre Harrsjön, the BlueMinerva operation did not generate significant surface waves or flow perturbations.

Furthermore, we determined a maximum water speed in the slipstream centerline of the propeller of roughly 44 m s^{-1} ($Re = 4.9 \cdot 10^6$), which decayed to 5 m s^{-1} in the jet centerline at a distance of 0.95 m at the chamber. This estimate can be considered very conservative, given jet spreading and turbulent mixing, causing the effective flow at the chamber to be considerably lower. In this setting, the propeller-induced flow likely only affected the downstream region of the thrusters. The chamber was positioned such that residual slipstream velocities decayed substantially before reaching the measurement area. When located upstream of the thrusters, the propeller influence on the water surface was likely even smaller. Hence, local turbulence from the propellers is unlikely to influence flux measurements substantially.

2.5.4 Payload and floating devices

According to the manufacturer recommendations, the maximum payload of the BlueBoat is 15 kg. However, the payload for the BlueMinerva amounted to 42.5 kg. To counteract the concomitant reduction in freeboard (height between the waterline and the top of the hull) and increasing draft, we installed four additional custom-fabricated floats made of polyvinyl chloride (PVC) tubes that were sealed on both ends (Fig. 3). Each float measured 96 cm in length and 11.5 cm in width. They were fitted to sit below the waterline to create maximum buoyancy and offset the additional weight. This configuration ensured stability and robustness of the platform during deployment, even when intermittent wind bursts exceeding 30 m s^{-1} occurred.

https://doi.org/10.5194/egusphere-2026-2262
Preprint. Discussion started: 26 May 2026

2.6 Data processing

2.6.1 BlueMinerva

While dry mole fractions measured with the LI-7810 did not require any corrections, the wet CO_2 mole fractions measured with the GMP343 were corrected online for temperature, humidity and pressure measured within the chamber. The respective data were transmitted to the datalogger via serial communication (RS232). Our chamber flux measurements usually lasted around 5 min. For one mission at Dagow Lake, we shortened the duration of measurements to 1.5 min to compare the sensor performance at shorter measurement intervals. For this mission, measurement locations were distributed across the lake to maximize spatial separation and to stress-test the motor by operating it over longer travel distances.

For simplicity, all fluxes (F) were estimated with Eq. 5 using linear regressions fitted to the change of dry CO_2 and CH_4 mole fractions over time ($\frac{dC}{dt}$), so that

$$F = \frac{dC}{dt} \cdot \frac{V}{A} \cdot \frac{p}{R \cdot T} \tag{5}$$

with the chamber volume (V) in m^3, chamber area (A) in m^2, measured barometric pressure (p) in Pa, the ideal gas constant (R$= 8.31$ m^3 Pa K^{-1} mol^{-1}), and the measured air temperature in the chamber (T) in K. Fluxes of CO_2 and CH_4 were discarded where the boat exceeded a speed of 0.25 m s^{-1} over, in total, ten or more seconds during individual measurements ($n = 9$). This occasionally occurred, for example, at the end of missions when the chamber measurement was still ongoing despite us manually maneuvering the BlueMinerva towards the lake shore. One measurement at Inre Harrsjön was disrupted by bubbles entering the chamber (ebullition), which was detected by an abrupt, large increase of mole fractions during the measurement. Consequently, we discarded the respective CO_2 and CH_4 flux. All other CO_2 fluxes were kept. Fluxes of CH_4 were discarded where $R^2 < 0.8$ ($n = 22$) and where bubbles entered the chamber and caused a sudden jump in CH_4 mole fractions, but not for CO_2 ($n = 1$). As a result, we obtained 485 flux estimates for CO_2 and 462 for CH_4 across Dagow Lake and Inre Harrsjön over 72 measurement hours in total.

Measured wind speeds were corrected for pitch and roll of the BlueMinerva, and were transformed into its reference frame (0° or north at the bow). The true wind speed was obtained by subtracting the GPS-derived velocity from the transformed and tilt-corrected wind speed.

For the multiparameter sonde, the wiping period (first 30 s of each hour) was discarded for the optical variables (DO, fDOM, chlorophyll, phycocyanin, turbidity). Furthermore, fDOM was corrected for temperature and light attenuation following Eq. 1-3 in Snyder et al. (2018).

Water depth was filtered based on the instrument-specific output of confidence levels, so that all depths above a confidence of 76% were retained. To delineate the lake outlines, we manually digitized polygons for each studied lake (https://geojson.io). To yield smoothed bathymetry for the whole lake, we assumed a virtual water depth of 0.1 m at distances of 0.5 m along all lake shores to ensure a shallow water depth towards the edges of the polygons. A 1 m by 1 m grid was generated across the water surface, and using triangulated linear interpolation embedded in the verde package in Python (Uieda, 2018), we interpolated the measured water depths. Based on residuals at grid cell level, this approach yielded a root mean squared error (RMSE) of

https://doi.org/10.5194/egusphere-2026-2262
Preprint. Discussion started: 26 May 2026

0.10 m for the water depth at Dagow Lake for 118,106 effectively measured points, and an RMSE of 0.11 m at Inre Harrsjön for 57,318 depth measurements.

2.6.2 Eddy covariance tower

At Dagow Lake, eddy covariance measurements were conducted at 20 Hz and processed with the software EddyPro (LI-COR Biosciences, 2021; Fratini and Mauder, 2014) to calculate half-hourly fluxes. A two-step coordinate rotation was applied to the three-dimensional wind vector measured with an ultrasonic anemometer (Gill HS-50, Gill Instruments Limited, UK). The gas concentration time series were linearly detrended to extract turbulent fluctuations and de-lagged relative to the vertical wind velocity to maximize covariance. Calculated CH_4 fluxes were corrected with respect to air density and water vapor dilution effects (Burba et al., 2012), and signal attenuation in the high- and low-frequency part of the turbulence spectrum (Fratini et al., 2012; Moncrieff et al., 2004). Finally, quality flags were generated according to Foken and Wichura (1996) and Sabbatini et al. (2018). Only data of the highest quality class were used for analyses. The fetch length that contributed 90% of the half-hourly flux was calculated based on Kljun et al. (2004) in order to determine if measurements of the BlueMinerva were taken within the tower footprint, or if the footprint extended beyond the lake surface.

2.7 Statistical analyses

We assessed the agreement of CO_2 fluxes between the two gas analyzers: the costlier LI-7810 and the lower-cost GMP343. We used a Bland-Altman plot to determine whether one of the analyzers consistently over- or underestimated the other, or whether their agreement changed with flux magnitude (Martin Bland and Altman, 1986).

When comparing the fluxes at Dagow Lake measured with the BlueMinerva and the eddy covariance tower, we selected data with the highest quality flag (0) from May 13-16, 2025 for the tower. In addition, we used the 90% fetch lengths and wind directions to identify the maximum extent of the footprint – depending on whether this location was on water or land, respectively, we removed any tower fluxes that were influenced by the land area. For the comparison between BlueMinerva and eddy tower, only EC fluxes with fetch lengths within the lake, and BlueMinerva measurements inside the footprint area were used. To test for significant differences ($p < 0.05$) between flux distributions from both methods, we used a nonparametric Mann-Whitney U test given that the datasets were independent, and reported the rank-biserial correlation coefficient (r_{rb}).

To determine spatial differences of carbon fluxes, we used standard statistics (median, 25th–75th percentiles, skewness of data distribution γ (Zwillinger and Kokoska, 2000)). To check whether meteorological, physicochemical, biological, and flux measurements were spatially structured and not randomly distributed, we determined the global Moran's I values (Moran, 1950) for each lake using k-nearest neighbors with row-standardized weights using libpysal and esda Python libraries (Rey and Anselin, 2010). The k was chosen to be 5 for Dagow Lake and 8 for Inre Harrsjön. The significance of Moran's I was evaluated using permutation tests with 999 random permutations, with $p < 0.05$ indicating a significant result. Similarly, the local Moran's I was determined and the quadrant of the Moran scatterplot was used to assign fluxes to spatially coherent hotspot and coldspot clusters ($p < 0.05$). These clusters represent locations where fluxes were consistently higher or lower than the lake-wide mean, and were embedded within neighborhoods of similarly high or low fluxes.

https://doi.org/10.5194/egusphere-2026-2262
Preprint. Discussion started: 26 May 2026

To visualize spatially continuous flux maps, the measurements were interpolated onto a regular grid using Gaussian kernel smoothing. To account for differences in lake areas, a grid size of 5 m was chosen for Dagow Lake and 1 m for Inre Harrsjön. For each grid cell within the lake polygon, flux values were computed as distance-weighted averages of nearby observations. The spatial smoothing length scale (σ) was chosen individually for each lake based on the typical spacing between measurement locations and their characteristic spatial scale of variability observed in the data ($\sigma = 30$ m at Dagow Lake, $\sigma = 10$ m at Inre Harrsjön). All analyses were conducted using Python (version 3.12.11).

3 Results and discussion

3.1 Comparison between analyzers and measurement duration

We compared the estimated CO_2 fluxes between the gas analyzers LI-7810 and GMP343 based on the measurements at Dagow Lake for the two measurement durations of approximately 5 min and 1.5 min (Fig. 5). For the duration of 5 min, the CO_2 flux estimates matched better between the analyzers (RMSE $= 0.04$ μmol m^{-2} s^{-1}) than for 1.5 min (RMSE $= 0.19$ μmol m^{-2} s^{-1}; Fig. 5A). Besides, the coefficient of determination (R^2) for fitting a linear function to estimate the CO_2 flux yielded better fits for the LI-7810 than for the GMP343 for both measurement durations (Fig. 5B). The Bland-Altman plots clearly show higher 95% limit bands for the short measurement duration (1.5 min; Fig. 5C) than for the longer measurement period (5 min; Fig. 5D). In addition, the trend in panel C indicates a bias proportional to the flux magnitude, which is substantially smaller in panel D. Overall, this implies that the higher precision of the LI-7810, compared to the GMP343, reduces uncertainties in flux estimates, but this advantage is marginal for longer sampling times. Nonetheless, the mean absolute difference between the flux estimates based on GMP343 and LI-7810 was very close to zero (0.001 μmol m^{-2} s^{-1}) for 1.5 min, and slightly larger for 5 min (-0.01 μmol m^{-2} s^{-1}). Therefore, even for shorter measurement periods, fluxes matched well on average. However, both sensors showed better agreement for longer measurement periods of 5 min.

As a result, we recommend a measurement period of 5 min rather than 1.5 min for future aquatic chamber measurements with the GMP343 or LI-7810. Besides, these findings suggest that aquatic CO_2 flux estimates based on 5 min long measurements agreed well between the GMP343 and LI-7810. Therefore, for future measurements requiring accurate CO_2 flux estimates with a similar setup as presented in this study, the lower-cost GMP343 can be considered sufficient. An additional incentive is the lower weight of the GMP343, which contributes to a smaller payload compared to the heavier LI-7810. However, if simultaneous measurements of CH_4 are required, the LI-7810 is a very suitable choice, given its high precision needed for comparatively short measurement cycles (5 min), as well as for measuring mole fractions close to atmospheric levels and resulting low fluxes in natural ecosystems. Alternative low-cost sensors (Bastviken et al., 2020; Malerba et al., 2025) may not be suitable for the current setup of the BlueMinerva due to their lower accuracy in the order of ppms, and the related requirement of long measurement durations. Accordingly, these sensors provide a good choice for stationary, long-term monitoring of aquatic fluxes.

https://doi.org/10.5194/egusphere-2026-2262
Preprint. Discussion started: 26 May 2026

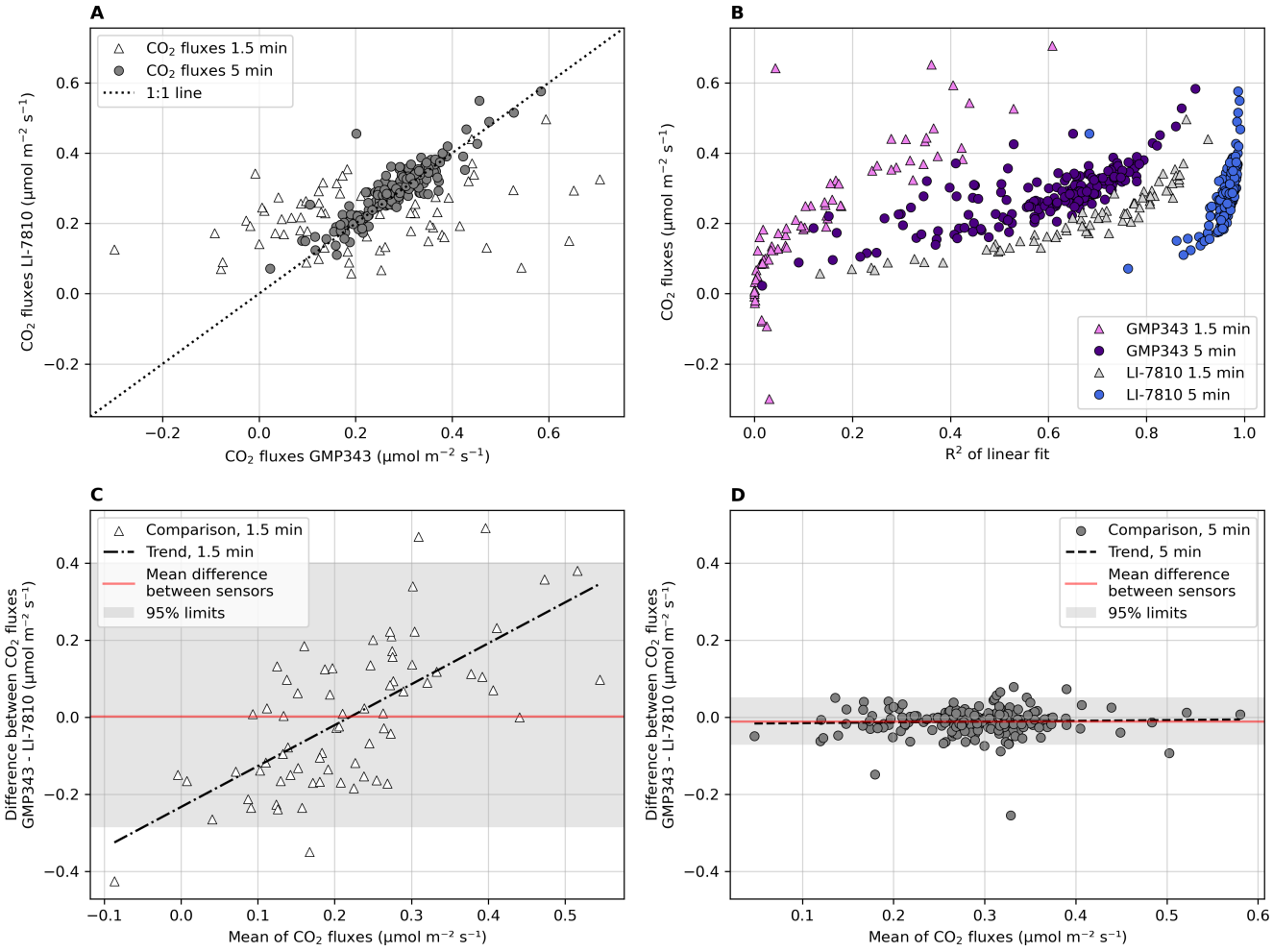

Figure 5. Estimated CO_2 fluxes at Dagow Lake for two gas analyzers: LI-7810 (LI-COR) and CARBOCAP GMP343 (Vaisala). In panel A, fluxes are directly compared between analyzers for measurement periods of 1.5 and 5 min. In panel B, all fluxes are shown with their corresponding R^2 of the linear fit. The lower panels are Bland-Altman plots to indicate the agreement between the analyzers for 1.5 min (panel C) and 5 min measurements (panel D).

3.2 Comparison between eddy covariance and chamber fluxes

305 Based on the results from the sensor intercomparison, for subsequent analyses in this study, we focused on flux estimates obtained with the LI-7810 only. Given that an eddy covariance tower equipped with a CO_2 and a CH_4 analyzer was located in the center of Dagow Lake, we compared the point-level chamber-based measurements taken with the BlueMinerva (Chamber) with the ecosystem-level measurements from the tower (EC). Such comparisons have been done previously at other lakes (Schubert et al., 2012; Podgrajsek et al., 2014; Erkkilä et al., 2018).

https://doi.org/10.5194/egusphere-2026-2262
Preprint. Discussion started: 26 May 2026

After selecting the flux estimates from within the same footprint area inside the lake during the measurement period of May 13–16, 2025 (Fig. B1), we did not find significant differences of CO_2 fluxes between EC and Chamber (Mann–Whitney U $= 287$, $p = 0.52$; Table 3). The rank-biserial correlation coefficient ($r_{rb} = 0.11$) indicated a small effect size and no substantial systematic difference between methods. However, in the case of CH_4, mean fluxes from the chamber setup were more than three times higher than from the tower (Table 3). These observed differences were significant (Mann–Whitney U $= 23$, $p < 0.01$), and the effect size was large ($r_{rb} = 0.91$). In previous studies, such discrepancies were linked with the higher spatial heterogeneity of CH_4 fluxes compared to CO_2 (Natchimuthu et al., 2016; Denfeld et al., 2020) and a resulting lack of spatial representativeness of EC measurements. Overall, it should be noted that CH_4 fluxes measured at Dagow Lake in May were low compared to estimates from the peak emission period later in the year. In line with this, not accounting for ebullition events for chamber measurements – bubbling was only detected on one occasion and the respective flux was excluded during data processing – likely did not affect overall CH_4 flux magnitudes given presumably small ebullition fluxes in spring (Praetzel et al., 2021). Therefore, discrepancies of CH_4 fluxes could be attributed to sensor-based differences resulting from a comparison between an open-path sensor for EC and a closed-path setup for the chamber (Detto et al., 2011). In addition, estimates of fetch length may have been subject to bias, given the non-homogeneous terrain and differences in roughness between the water surface and the mature forest surrounding the lake, which may have led to a stronger influence of terrestrial signals for EC fluxes than suggested by the footprint estimates. If we assumed near-zero CH_4 fluxes or even uptake from the surrounding forest (Lang et al., 2025), the result could be an underestimation of lake CH_4 fluxes by EC.

Regarding previous intercomparisons between fluxes from EC and floating chamber systems, the cumulative CH_4 flux derived from floating chamber measurements was lower than from EC measurements at a Swiss lake (Schubert et al., 2012). Similarly, at a lake in southwest Sweden CH_4 fluxes based on chambers were substantially lower than from EC measurements, in this case likely due to different footprints that captured higher-emitting areas with EC (Podgrajsek et al., 2014). However, findings from a lake in southern Finland showed higher CH_4 flux estimates for chambers than for EC (Erkkilä et al., 2018), similar to results found in this study. This was justified by overall low CH_4 fluxes which may have fallen below EC detection limits. A similar effect may have affected our method intercomparison for Dagow Lake, given that previous studies found a minimum detection limit around 3 nmol m^{-2} s^{-1} for the open-path analyzer LI-7700 used in the EC setup (Detto et al., 2011; Deventer et al., 2019). However, this potential effect would not fully explain the flux discrepancies between methods. At the same time, CO_2 fluxes in Erkkilä et al. (2018) matched similarly well between methods as found in this study.

3.3 Meteorological, physicochemical, and biological measurements

Meteorological variables including air temperature, relative humidity, barometric pressure and wind speed varied widely when averaged during measurements at Dagow Lake and at Inre Harrsjön (Fig. 6). Given that measurements at Inre Harrsjön were taken a week apart with warmer temperatures in the second half of the campaign, water temperatures showed a clear bimodal distribution. Due to the temperature dependence of pH (Langelier, 1946), we found large spatial variability within Inre Harrsjön for this variable, while measurements were rather stable at Dagow Lake. Also dissolved oxygen, chlorophyll and phycocyanin concentrations showed more variability at Inre Harrsjön than at Dagow Lake. Furthermore, substantial differences in magni-

https://doi.org/10.5194/egusphere-2026-2262
Preprint. Discussion started: 26 May 2026

Table 3. Comparison of CO_2 and CH_4 fluxes between eddy covariance (EC) and chamber measurements for May 13–16, 2025 at Dagow Lake. Fluxes from EC and chambers were filtered to include only those within the 90% footprint area around the EC tower (see Fig. B1). For EC, the footprint where 90% of the data contributed to the flux was used, and only fluxes with the best quality flag were selected. The number of observations (n) refers to half-hourly fluxes for EC and to individual measurements for chambers.

Statistics	CO_2 fluxes (μmol m^{-2} s^{-1})		CH_4 fluxes (nmol m^{-2} s^{-1})	
	EC	Chamber	EC	Chamber
n	38	17	29	17
Mean	0.03	0.27	5.25	18.96
Std.	1.31	0.11	3.61	7.17
Min.	-1.74	0.06	-2.62	5.90
Median	-0.27	0.29	4.84	19.24
Max.	2.82	0.49	13.28	33.00

tudes of specific conductivity (359–364 μS cm^{-1} at Dagow Lake and 62–63 μS cm^{-1} at Inre Harrsjön) and fDOM (14–24 QSU at Dagow Lake and 53–58 QSU at Inre Harrsjön) were identified between the test lakes. We also found that all environmental variables differed significantly between measurement days (Kruskal-Wallis test, $p < 0.05$; Fig. C1), and that all variables exhibited significant spatial structure within both lakes (global Moran's I ranging between 0.06–0.74, $p < 0.05$; Table S1). This pronounced spatial and temporal variability in environmental conditions suggests that a highly resolved monitoring program, such as made possible by the BlueMinerva platform, is necessary to capture a representative net carbon flux for such ecosystems. With our flux measurements conducted under a wide range of environmental conditions and in a heterogeneous spatial context, we established a suitable basis for flux measurements across contrasting local conditions.

3.4 Spatial heterogeneity of carbon fluxes

Fluxes of CO_2 measured with the BlueMinerva ranged from 0.06 to 0.58 μmol m^{-2} s^{-1} at Dagow Lake (n = 250), and from -0.48 to 0.25 μmol m^{-2} s^{-1} at Inre Harrsjön (n = 235, Fig. 7A and C). Fluxes of CH_4 varied between 4.38 and 48.91 nmol m^{-2} s^{-1} at Dagow Lake (n = 249), and between 1.99 and 35.08 nmol m^{-2} s^{-1} at Inre Harrsjön (n = 213, Fig. 7B and D).

In a previous study at Dagow Lake, negative CO_2 fluxes very close to zero were found between 2006 and 2007 (-0.01–0.18 μmol m^{-2} s^{-1}), and a small source of CH_4 (0.46–7.06 nmol m^{-2} s^{-1}) was quantified from water surface flask samples using gas transfer parameterizations (Casper et al., 2009). For lakes in the Stordalen catchment, mean ice-free season fluxes of 0.17 $\pm$ 0.11 μmol m^{-2} s^{-1} for CO_2 and 8.67 $\pm$ 5.78 nmol m^{-2} s^{-1} for CH_4 were determined from water samples and estimated gas transfer (Lundin et al., 2013). Specifically for Inre Harrsjön, CH_4 ebullition was captured with ebullition traps and fluxes reached up to 567 nmol m^{-2} s^{-1}, but 4.91 nmol m^{-2} s^{-1} on average (Wik et al., 2013). These magnitudes of fluxes agreed well

https://doi.org/10.5194/egusphere-2026-2262
Preprint. Discussion started: 26 May 2026

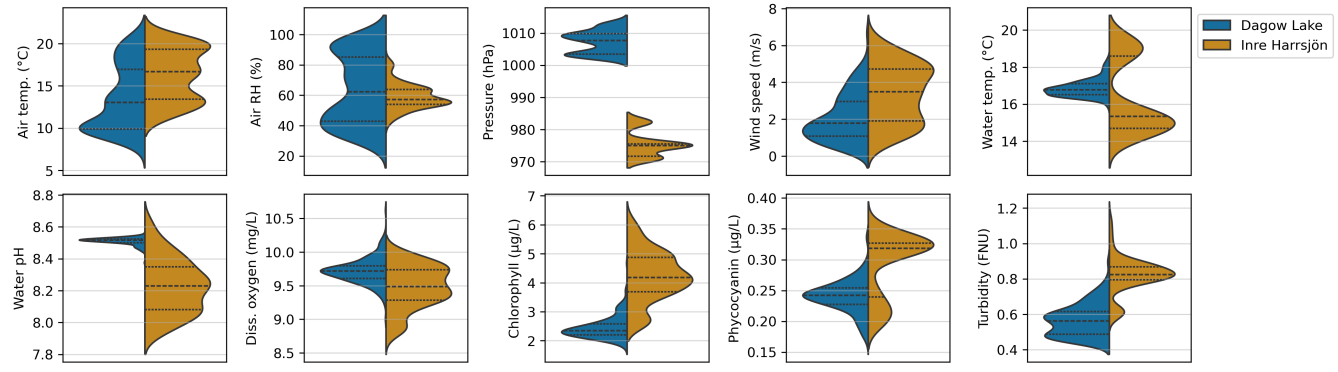

Figure 6. Violin plots of meteorological variables (air temperature, relative humidity, barometric pressure, and wind speed) and physicochemical and biological variables (water temperature, pH, dissolved oxygen concentration, chlorophyll and phycocyanin concentrations and turbidity) during measurements at Dagow Lake and Inre Harrsjön. For better visibility, two outliers of turbidity at Dagow Lake were removed. Specific conductivity and fluorescent DOM measurements are not shown.

with those determined with the BlueMinerva in our study. However, none of the previous measurement campaigns resolved the fluxes spatially as detailed as the BlueMinerva did within a matter of a few days (Fig. 7).

The distribution of CO_2 flux rates at Dagow Lake was largely symmetric around the median (0.28 μmol m^{-2} s^{-1}, 25th–75th percentiles: 0.22–0.33 μmol m^{-2} s^{-1}), and the data distribution was almost unskewed ($\gamma = 0.09$), indicating moderate spatial variability. Our spatially distributed dataset indicated highest fluxes occurring in the southwestern tip of the lake (Fig. 7A and 8A). For CH_4, highest fluxes were detected at the northeastern shore, which led to a slight positive skew ($\gamma = 0.39$) and a more pronounced spatial heterogeneity compared to CO_2 (median: 20.15 nmol m^{-2} s^{-1}, percentiles: 15.13–24.38 nmol m^{-2} s^{-1}; Fig. 7B and 8B). At Inre Harrsjön, slightly negative CO_2 fluxes prevailed (median: -0.06 μmol m^{-2} s^{-1}, percentiles: -0.16–0.01 μmol m^{-2} s^{-1}), causing a negative skew ($\gamma = -0.30$). The highest uptake was measured towards the southern shore alongside the highest emission (Fig. 7C and 8C). However, since measurements were taken in two blocks a week apart from each other, the emerging spatial patterns may also be influenced by temporal differences. Slight spatial heterogeneity was also found for CH_4, with a mild positive skew ($\gamma = 0.25$, median: 14.83 nmol m^{-2} s^{-1}, percentiles: 9.64–18.62 nmol m^{-2} s^{-1}), and highest fluxes close to the southern shore (Fig. 7D and 8D). At Inre Harrsjön, we spared the eastern shore from measurements due to the dense growth of emergent horsetail, in order to prevent damage to the plants and disruption to the missions (Fig. 7C and D).

Our geostatistical analyses revealed that fluxes were not randomly distributed in space in either lake, for either gas. For CO_2 fluxes, we found weak, but significant positive autocorrelation at Dagow Lake (k = 5, Moran's I = 0.12, $p < 0.01$) and at Inre Harrsjön (k = 8, Moran's I = 0.10, $p < 0.01$), which suggests patchy structure at small spatial scales. For CH_4, fluxes were just slightly more autocorrelated at Dagow Lake (k = 5, Moran's I = 0.13, $p < 0.01$), but showed the strongest spatial autocorrelation at Inre Harrsjön (k = 8, Moran's I = 0.33, $p < 0.01$). Consequently, CH_4 fluxes at Inre Harrsjön were organized into distinct spatial clusters, indicating the presence of coherent high- and low-flux regions rather than scattered hotspots

https://doi.org/10.5194/egusphere-2026-2262
Preprint. Discussion started: 26 May 2026

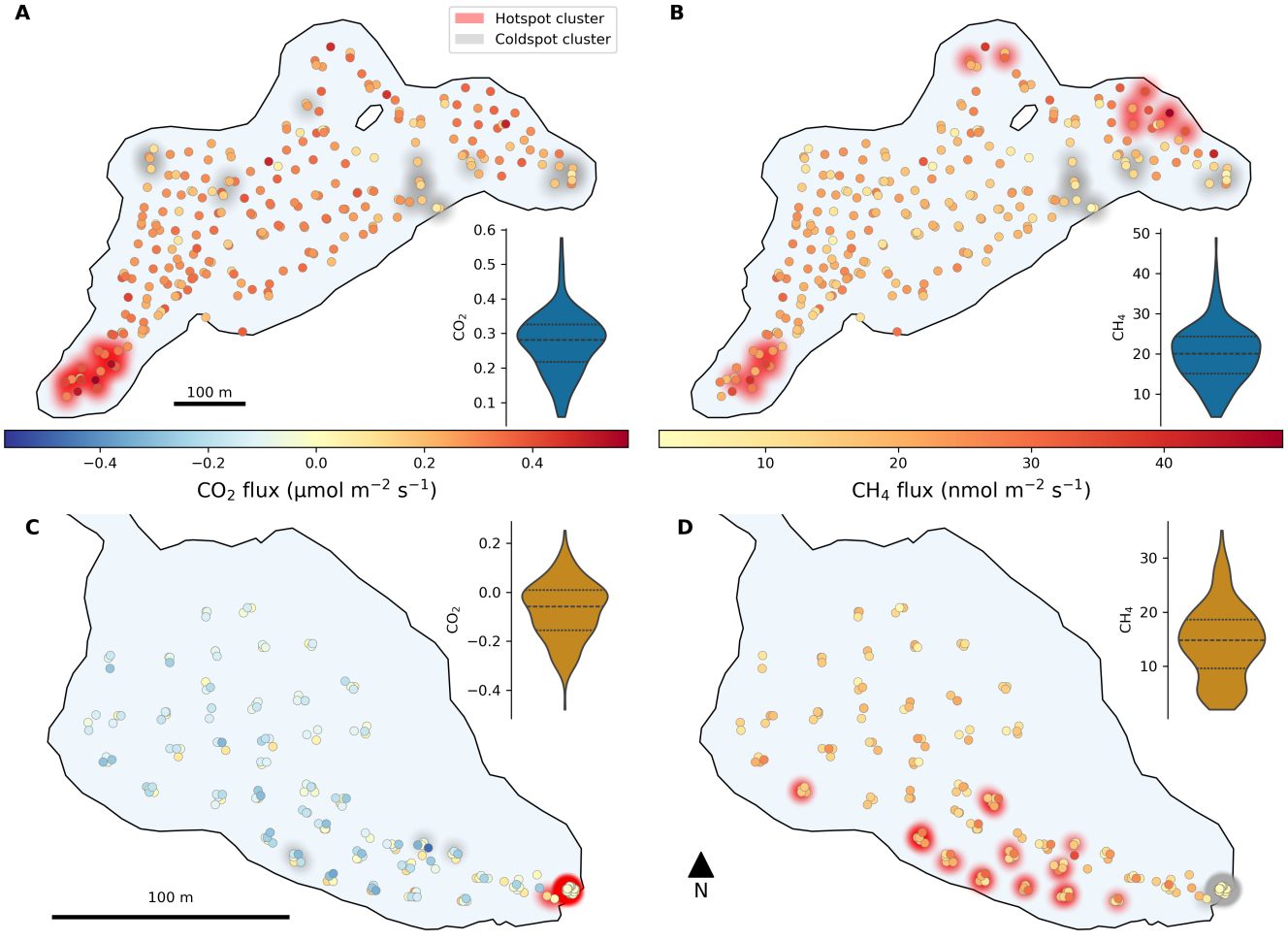

Figure 7. Spatially-resolved fluxes of CO_2 (panels A and C) and CH_4 (B and D) measured at Dagow Lake (A and B) and at Inre Harrsjön (C and D). Uptake of CO_2 (negative flux) was only measured at Inre Harrsjön. Violin plots show the distribution of CO_2 and CH_4 fluxes per lake, and the median with 25th and 75th percentiles. Halos around points indicate lake-specific clusters of hot and coldspots, as determined by local Moran's I.

(Fig. 7D). These results demonstrate that the spatial variability of fluxes was structured, underscoring the critical limitation of traditional sampling approaches to capture or represent true spatial patterns. Our autonomous platform, by contrast, enables systematic, high-resolution spatial mapping of fluxes (Fig. 8) – providing a methodological solution to a long-standing sampling bias.

https://doi.org/10.5194/egusphere-2026-2262
Preprint. Discussion started: 26 May 2026

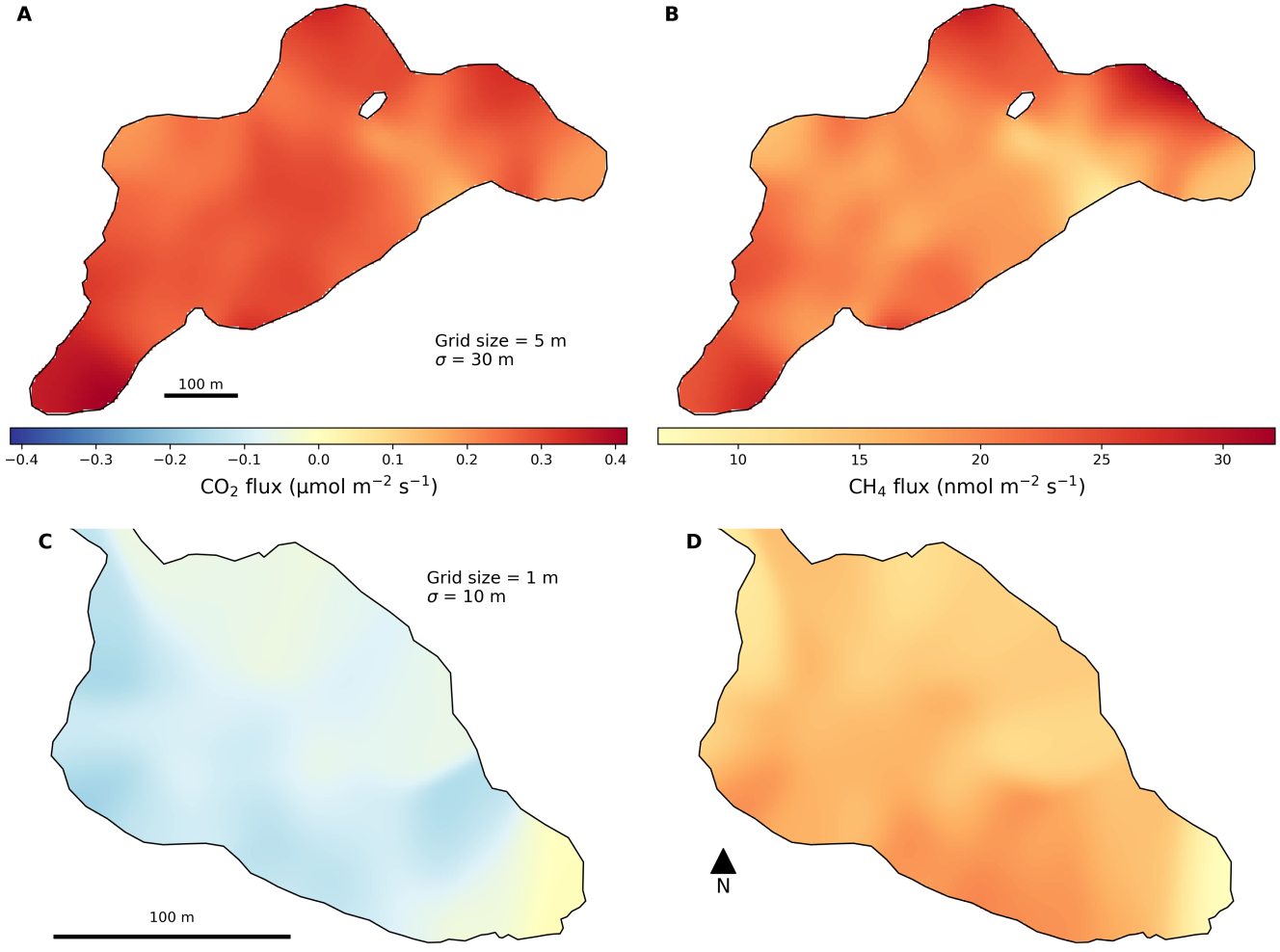

Figure 8. Spatially continuous maps of CO_2 (panels A and C) and CH_4 fluxes (B and D) for Dagow Lake (A and B) and Inre Harrsjön (C and D). Spatial flux maps were generated using Gaussian kernel smoothing of measured data. Grid sizes and spatial smoothing length scales (σ) differed between lakes and were kept small to avoid over-smoothing and preserve spatially heterogeneous patterns.

4 Limitations and opportunities

The ability of the BlueMinerva to collect data at small scales across waterbodies with consistent protocols provides the spatial density required to resolve meaningful CO_2 and CH_4 flux variability – something most prior studies cannot achieve. In the following, we list some limitations of the outlined setup and suggest directions for future developments.

https://doi.org/10.5194/egusphere-2026-2262
Preprint. Discussion started: 26 May 2026

4.1 Practical considerations

Pre-measurement inspection: To facilitate the planning of the measurement missions, the software Mission Planner (ArduPilot Dev Team, 2024) provides background satellite imagery on a global level. Depending on its recency, the imagery may be more or less accurate. To mitigate the risk of the platform being hindered by obstacles, it is always recommended to inspect the target area prior to starting a mission for emergent vegetation that may become entangled in the propellers, or for very shallow areas, as well as submerged and exposed rocks in the lakes that may ground the platform. In addition, the platform may pose potential risks to human swimmers and traffic on the water. Therefore, an autonomous operation is only possibly if the waterbody shows no further human use, or if all users have been instructed accordingly.

Deployment in shallow waters: The BlueMinerva has a draft of roughly 23 cm. Therefore, it is recommended to deploy the platform using this setup at a minimum water depth of roughly 25 cm. Consequently, maneuvers towards shallow lake shores, but also subaqueous features (shoals, sandbanks, rock outcrops, or submerged dense vegetation beds) should be undertaken with caution.

Deployment in turbulent waterbodies: We recommend to use the BlueMinerva in the present setup on lakes or low-flow waterbodies only. While the BlueBoat was developed for any waterbody, including marine ecosystems, we refrained from testing the setup in such waterbodies to mitigate the risk of damaging instruments and electronic parts. Besides, under high-energy circumstances, waves may develop and lead to air intrusion into the water-sealed chamber, thereby compromising the measurement. The BlueMinerva was occasionally exposed to short wind bursts exceeding 30 m s^{-1} during measurements, but withstood these conditions without issues. In fluvial waterbodies, the missions would need to be adapted, since it would potentially not be possible to maintain the measurement location during loitering due to the presence of currents. Furthermore, autonomous measurements would not be possible due to the likelihood of obstacles such as fallen trees, rocks, cascades and boats.

Weight: The total weight of the BlueMinerva in the configuration described above was 57 kg. Managing such a weight can be challenging and may require several people to assist in the field. Ideally, the platform would be transported to the target lake by vehicle. Alternatively, the components of the platform can be carried individually to the target area which is less efficient in terms of time and workforce. One optional item with a high impact on the overall payload is the LI-7810 with internal batteries (10.5 kg). The case which houses the datalogger and further electronics (9 kg) also significantly contributes to the total weight of the platform. As shown here, the GMP343 is a lighter-weight, reliable alternative to the heavier LI-7810 for those only interested in CO_2, and not CH_4 flux patterns.

Depth profiles: The main focus of the BlueMinerva is to capture surface processes with high spatial coverage. Nonetheless, processes within the water column should not be neglected as they are closely coupled to surface dynamics through vertical mixing and physical stratification, with direct implications for carbon exchange, biological productivity, and nutrient availability (Bastviken et al., 2008). Therefore, depth profiles can be conducted manually using the multiparameter sonde mounted on the BlueMinerva, which is done by slowly lowering the sonde into the water. This is only possible if

https://doi.org/10.5194/egusphere-2026-2262
Preprint. Discussion started: 26 May 2026

the BlueMinerva is not operating autonomously and a small rowing boat or similar vessel is available. Ideally, the profile is conducted at a location where the waterbody is deepest. An example for Dagow Lake can be found in the appendix, Fig. E1.

4.2 Potential upgrades

Some technical upgrades could transform the BlueMinerva from a capable autonomous platform into a truly adaptive and resilient system for aquatic biogeochemical monitoring.

Battery life: The bottleneck of the battery setup used for the BlueMinerva are the LI-7810 batteries. The endurance of the remaining components powered by the other batteries (Table 2) is higher. Therefore, adding extra power sources for operating the LI-7810 would extend the duration of gas measurements, and therefore the duration of the missions overall. However, this would come at the expense of increased overall weight. Ultimately, the best compromise between payload, power supply and operation needs to be identified on a case-by-case basis.

Additional variables: While the BlueMinerva captures a large portion of relevant variables, more variables could be added to deepen our understanding of factors driving surface fluxes. Setting aside drawbacks related to weight, further meaningful aquatic measurements that could be added in future setups include those of dissolved gas and dissolved organic carbon concentrations. Combining the BlueMinerva with previously developed systems (Crawford et al., 2015; Dalvai Ragnoli and Singer, 2024; Zug et al., 2025) could potentially complement the array of obtainable measurements, both at the surface and subsurface. Furthermore, the modular design of the platform enables the measurement of other trace gases by replacing the CO_2 and CH_4 analyzers with sensors tailored to measure, for instance, nitrous oxide, or volatile organic compounds.

Adaptive, data-driven path planning: While the BlueMinerva currently operates along fully pre-programmed trajectories, future upgrades could incorporate real-time spatial modeling – such as Gaussian process regression over observed flux gradients – to enable the platform to dynamically adjust its sampling strategy. This would allow high-flux regions to be revisited at higher resolution, and anomalies to trigger adaptive responses, significantly improving flux budget accuracy without increasing deployment time. Such information-driven navigation is an active area of mobile robotics research and represents a natural next step toward intelligent aquatic monitoring.

Heterogeneous multi-robot systems: Beyond single-platform deployments, integrating the BlueMinerva with complementary platforms – such as underwater vehicles for continuous depth profiling or aerial drones for large-scale spatial context – could address current limitations in vertical and spatial coverage. Coordinating these systems across different sensing modalities (individual, complementary, or tightly collaborative operation modes) would enable comprehensive, multi-scale monitoring of lake biogeochemistry, reducing reliance on manual interventions.

Onboard fault detection and recovery: Increasing the operational robustness of the BlueMinerva through real-time anomaly detection – such as chamber seal failure, propeller entanglement, collisions with submerged or floating objects, or po-

https://doi.org/10.5194/egusphere-2026-2262
Preprint. Discussion started: 26 May 2026

sition drift beyond acceptable thresholds – combined with defined recovery behaviors, would be essential for longer unattended deployments. This would improve data quality and reduce the need for human supervision, enhancing the platform's reliability in remote or challenging environments.

4.3 New opportunities

As this study showed, the BlueMinerva was operated in a near-continuous mode, collecting almost seven flux measurements per measurement hour. Once initiated, the platform operated unsupervised on the chosen lake domain and only required action when it was time to change batteries or when technical issues arose. During previous tests, the BlueMinerva was exposed to heavy rain, but measurements were not compromised.

Given this efficiency and robustness, the BlueMinerva is a promising tool to determine small-scale variability in carbon fluxes as well as physicochemical, biological, meteorological and bathymetric features of low-flow waterbodies and enables the acquisition of dense, spatially resolved datasets with minimal effort. The wide use of this and similar platforms has the potential to advance our understanding of carbon cycle processes in waterbodies tremendously – given that in an ideal scenario almost 170 flux measurements could be taken within a day, and over 1,000 within a week. These measurements are useful to generate snapshot maps of carbon emissions (Fig. 8), bathymetry and water quality which may be of interest to local communities, stakeholders, and policymakers. When used over longer periods, the BlueMinerva can provide extensive datasets, offering an unparalleled combination of highly resolved surface fluxes alongside waterbody and climate characteristics. This allows for new insights into control factors and functional relationships, which are often required to inform machine learning models aiming to improve predictive capability and reduce uncertainty in emission estimates.

Data availability. System files including the datalogger program and wiring diagram, an example mission file for the Mission Planner software, and a 3D animation of the BlueMinerva are available on Zenodo at https://doi.org/10.5281/zenodo.19136563 (Vogt et al., 2026a). The flux estimates with ancillary data, interpolated bathymetry, and the depth profile collected at Dagow Lake are available on Zenodo at https://doi.org/10.5281/zenodo.19365068 (Vogt et al., 2026b).

https://doi.org/10.5194/egusphere-2026-2262
Preprint. Discussion started: 26 May 2026

Appendix A: Trajectories of missions

The pre-programmed trajectories and measurement locations are shown in Fig. A1.

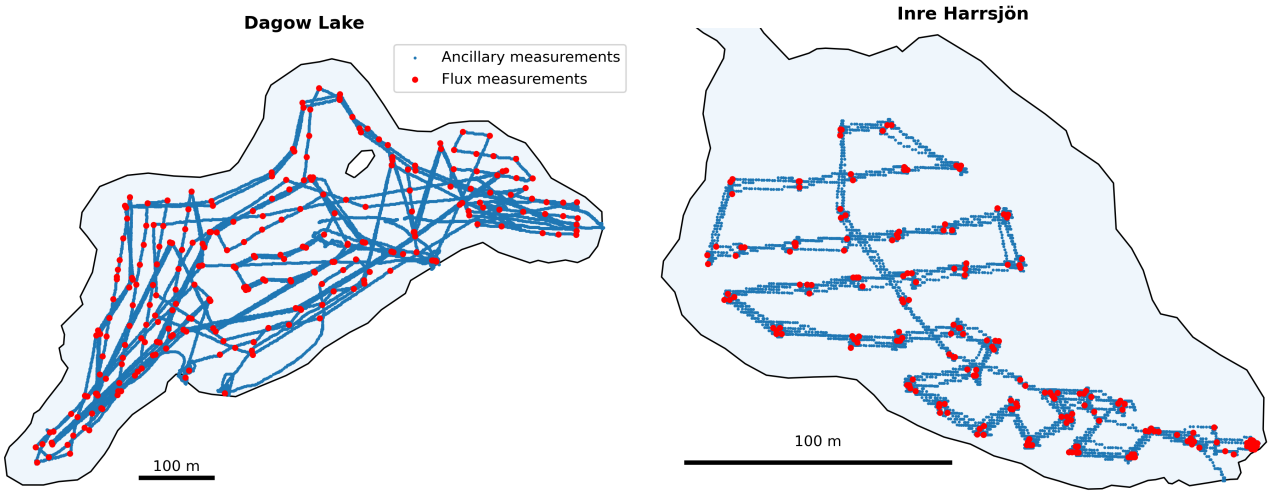

Figure A1. Trajectories and locations of ancillary and flux measurements at Dagow Lake and Inre Harrsjön.

https://doi.org/10.5194/egusphere-2026-2262
Preprint. Discussion started: 26 May 2026

Appendix B: Eddy covariance footprint and measurement locations of associated chamber fluxes

The flux measurements taken with the BlueMinerva that coincided with the footprint area of the eddy covariance tower at Dagow Lake during the measurement period are shown in Fig. B1.

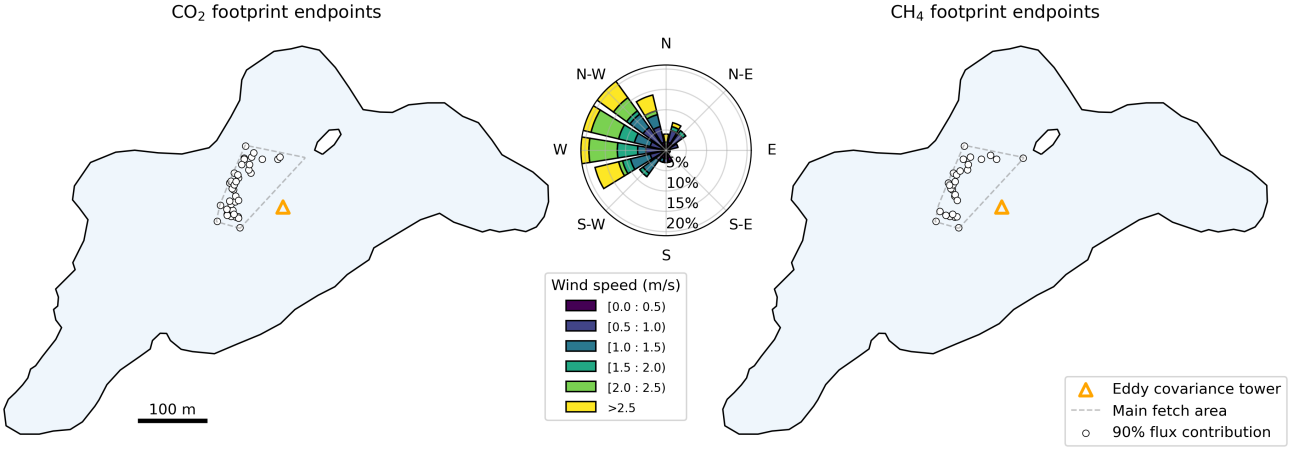

Figure B1. The flux measurements for CO_2 (left) and CH_4 (right) at Dagow Lake were placed on the map under consideration of the fetch length and the wind direction, where 90% of the data from within the given distance of the tower contributed to the measured flux. Only fluxes with the highest quality flag during the measurement period (May 13-16, 2025) were shown. The main fetch area denotes the area within the lake, where the fluxes were assumed to mainly originate from. The wind rose shows the wind speed and direction measured at the eddy covariance tower during the measurement period.

https://doi.org/10.5194/egusphere-2026-2262
Preprint. Discussion started: 26 May 2026

Appendix C: Daily timeseries of environmental variables

The daily variability of environmental variables measured alongside the carbon fluxes are shown in Fig. C1.

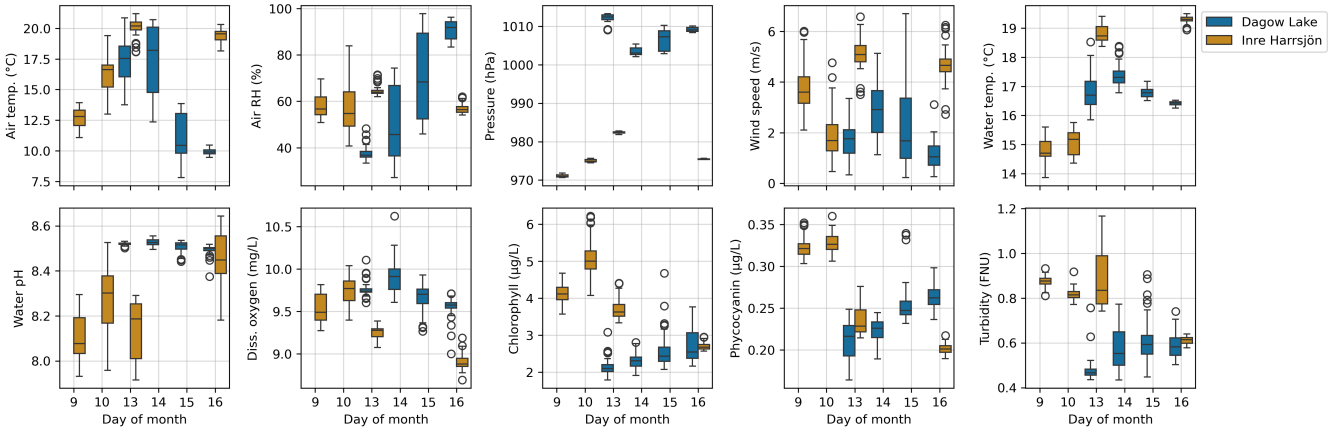

Figure C1. Boxplots of meteorological variables (air temperature, relative humidity, barometric pressure, and wind speed) and hydrochemical variables (water temperature, pH, dissolved oxygen concentration, chlorophyll and phycocyanin concentrations, and turbidity) for each measurement day at Dagow Lake (in May 2025) and Inre Harrsjön (in July 2025). For better visibility two outliers of turbidity at Dagow Lake were removed. Specific conductivity and fluorescent DOM measurements are not shown.

https://doi.org/10.5194/egusphere-2026-2262
Preprint. Discussion started: 26 May 2026

Appendix D: Global Moran's I for environmental variables

To determine the spatial autocorrelation of the environmental variables within each lake, we determined global Moran's I values (Fig. D1).

Table D1. Global Moran's I for each lake and environmental variable to determine spatial autocorrelation. Moran's I permutation tests were not significant ($p > 0.05$) for air humidity, chlorophyll, and fDOM at Inre Harrsjön and are therefore not shown.

Lake	Variable	Moran's I	p
Dagow Lake	Air temp.	0.34	< 0.01
	Air RH	0.16	< 0.01
	Pressure	0.47	0.02
	Wind speed	0.21	< 0.01
	Water temp.	0.09	0.01
	Water pH	0.38	< 0.01
	Diss. oxygen	0.43	< 0.01
	Chlorophyll	0.25	< 0.01
	Phycocyanin	0.20	< 0.01
	Turbidity	0.19	< 0.01
	Spec. conductivity	0.58	< 0.01
	fDOM	0.20	< 0.01
Inre Harrsjön	Air temp.	0.30	< 0.01
	Pressure	0.74	< 0.01
	Wind speed	0.08	< 0.01
	Water temp.	0.34	< 0.01
	Water pH	0.08	< 0.01
	Diss. oxygen	0.06	0.03
	Phycocyanin	0.21	< 0.01
	Turbidity	0.11	< 0.01
	Spec. conductivity	-0.08	< 0.01

https://doi.org/10.5194/egusphere-2026-2262
Preprint. Discussion started: 26 May 2026

Appendix E: Depth profile from Dagow Lake

The vertical distribution of water temperature, dissolved oxygen, pH and specific conductivity were obtained from depth profiles taken with the multiparameter sonde (Fig. E1).

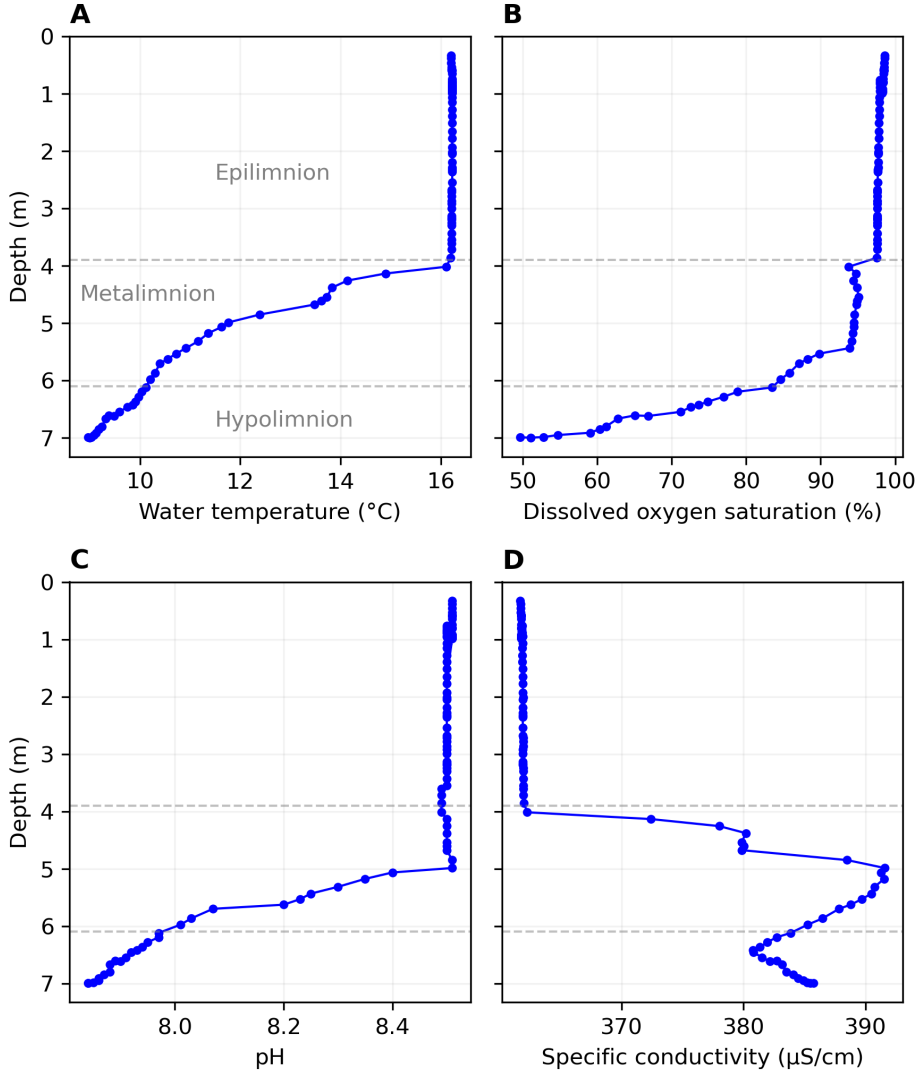

Figure E1. Depth profile taken with the multiparameter sonde at Dagow Lake (Latitude: 53.1516°N, Longitude: 13.0559°E) on May 16, 2025. Panel A shows the vertical water temperature profile, panel B dissolved oxygen saturation, panel C pH, and panel D specific conductivity. The water depth at the point of measurement was around 8 m. The depth of the epilimnion, metalimnion and hypolimnion were determined visually based on the water temperature profile.

https://doi.org/10.5194/egusphere-2026-2262
Preprint. Discussion started: 26 May 2026

Author contributions. JV and MG conceptualized the study. JV, TSEM, CB, MG co-designed the BlueMinerva guided by MPL, SZ and JM. TSEM and CB performed hardware integration and mechanical assembly. AB provided technical support with software configuration. JV and EP acquired the data. TS, CW, and MH processed and provided the eddy covariance data. JV curated the data, performed the formal analysis and prepared the original draft. MG acquired funding and supervised. All authors reviewed the manuscript.

Competing interests. The authors declare that they have no conflict of interest.

Acknowledgements. We thank Karel Castro-Morales and the Friedrich Schiller University in Jena for lending us the EXO2 Sonde. We thank István Héjja for producing the technical drawing of the BlueMinerva. We also acknowledge the help by Sanjid Backer Kanakkassery, Nicholas Eves, Martin Heimann, Kseniia Ivanova, Lara Oxley, Mark Schlutow, Nathalie Triches, Elias Wahl, and Theresia Yazbeck during field work, and acknowledge the support of the Workshops Service group at MPI-BGC. We thank Gero Licht (TU Bergakademie Freiberg) for technical advice and conceptual input on autonomous surface vehicle design and operation. We acknowledge the use of ChatGPT (GPT-5.3-mini model) to support coding, and deepl Write to improve text passages.

The authors acknowledge funding from the European Research Council (ERC synergy project Q-Arctic, grant agreement no. 951288) and from the Horizon Europe Climate programme (GreenFeedback project, grant agreement no. 101056921). The eddy covariance system on Dagow Lake is part of the Terrestrial Environmental Observatories Network (TERENO) of the Helmholtz Association of German Research Centres.

https://doi.org/10.5194/egusphere-2026-2262
Preprint. Discussion started: 26 May 2026

References

ArduPilot Dev Team: Mission Planner Ground control station software for ArduPilot, https://ardupilot.org/planner/, version 1.3.82, 2024.

Bastviken, D., Cole, J. J., Pace, M. L., and Van de Bogert, M. C.: Fates of methane from different lake habitats: Connecting whole-lake budgets and CH_4 emissions, Journal of Geophysical Research: Biogeosciences, 113, https://doi.org/10.1029/2007JG000608, 2008.

Bastviken, D., Nygren, J., Schenk, J., Parellada Massana, R., and Duc, N. T.: Technical note: Facilitating the use of low-cost methane (CH_4) sensors in flux chambers – calibration, data processing, and an open-source make-it-yourself logger, Biogeosciences, 17, 3659–3667, https://doi.org/10.5194/bg-17-3659-2020, 2020.

Burba, G., Schmidt, A., Scott, R. L., Nakai, T., Kathilankal, J., Fratini, G., Hanson, C., Law, B., McDermitt, D. K., Eckles, R., Furtaw, M., and Velgersdyk, M.: Calculating CO_2 and H_2O eddy covariance fluxes from an enclosed gas analyzer using an instantaneous mixing ratio, Global Change Biology, 18, 385–399, https://doi.org/10.1111/j.1365-2486.2011.02536.x, 2012.

Casper, P., Albino, M. F., and Adams, D. D.: Diffusive fluxes of CH_4 and CO_2 across the water-air interface in the eutrophic Lake Dagow, northeast Germany, SIL Proceedings, 1922-2010, 30, 874–877, https://doi.org/10.1080/03680770.2009.11902261, 2009.

Crawford, J. T., Loken, L. C., Casson, N. J., Smith, C., Stone, A. G., and Winslow, L. A.: High-Speed Limnology: Using Advanced Sensors to Investigate Spatial Variability in Biogeochemistry and Hydrology, Environmental Science & Technology, 49, 442–450, https://doi.org/10.1021/es504773x, 2015.

Dalvai Ragnoli, M. and Singer, G.: The River Runner: a low-cost sensor prototype for continuous dissolved greenhouse gas measurements, Journal of Sensors and Sensor Systems, 13, 41–61, https://doi.org/10.5194/jsss-13-41-2024, 2024.

Denfeld, B. A., Lupon, A., Sponseller, R. A., Laudon, H., and Karlsson, J.: Heterogeneous CO_2 and CH_4 patterns across space and time in a small boreal lake, Inland Waters, 10, 348–359, https://doi.org/10.1080/20442041.2020.1787765, 2020.

Desrosiers, K., DelSontro, T., and del Giorgio, P. A.: Disproportionate Contribution of Vegetated Habitats to the CH_4 and CO_2 Budgets of a Boreal Lake, Ecosystems, 25, 1522–1541, https://doi.org/10.1007/s10021-021-00730-9, 2022.

Detto, M., Verfaillie, J., Anderson, F., Xu, L., and Baldocchi, D.: Comparing laser-based open- and closed-path gas analyzers to measure methane fluxes using the eddy covariance method, Agricultural and Forest Meteorology, 151, 1312–1324, https://doi.org/10.1016/j.agrformet.2011.05.014, 2011.

Deventer, M. J., Griffis, T. J., Roman, D. T., Kolka, R. K., Wood, J. D., Erickson, M., Baker, J. M., and Millet, D. B.: Error characterization of methane fluxes and budgets derived from a long-term comparison of open- and closed-path eddy covariance systems, Agricultural and Forest Meteorology, 278, 107 638, https://doi.org/10.1016/j.agrformet.2019.107638, 2019.

Dietrich, Z. A., Savage, K. E., Atwood, A., Abrams, L. J., and Macedo, M. N.: AQUA-Flux: An Inexpensive, Autonomous Floating Chamber for High-Frequency, Long-Term Monitoring of Greenhouse Gas Fluxes From Aquatic Ecosystems, Journal of Geophysical Research: Biogeosciences, 130, e2025JG008 896, https://doi.org/10.1029/2025JG008896, 2025.

Dubey, R., Telles, A., Nikkel, J., Cao, C., Gewirtzman, J., Raymond, P. A., and Lee, X.: Low-Cost CO_2 NDIR Sensors: Performance Evaluation and Calibration Using Machine Learning Techniques, Sensors, 24, 5675, https://doi.org/10.3390/s24175675, 2024.

Dunbabin, M. and Grinham, A.: Quantifying Spatiotemporal Greenhouse Gas Emissions Using Autonomous Surface Vehicles, Journal of Field Robotics, 34, 151–169, https://doi.org/10.1002/rob.21665, 2017.

Erkkilä, K.-M., Ojala, A., Bastviken, D., Biermann, T., Heiskanen, J. J., Lindroth, A., Peltola, O., Rantakari, M., Vesala, T., and Mammarella, I.: Methane and carbon dioxide fluxes over a lake: comparison between eddy covariance, floating chambers and boundary layer method, Biogeosciences, 15, 429–445, https://doi.org/10.5194/bg-15-429-2018, 2018.

https://doi.org/10.5194/egusphere-2026-2262
Preprint. Discussion started: 26 May 2026

Foken, T. and Wichura, B.: Tools for quality assessment of surface-based flux measurements, Agricultural and Forest Meteorology, 78, 83–105, https://doi.org/10.1016/0168-1923(95)02248-1, 1996.

Fratini, G. and Mauder, M.: Towards a consistent eddy-covariance processing: an intercomparison of EddyPro and TK3, Atmospheric Measurement Techniques, 7, 2273–2281, https://doi.org/10.5194/amt-7-2273-2014, 2014.

Fratini, G., Ibrom, A., Arriga, N., Burba, G., and Papale, D.: Relative humidity effects on water vapour fluxes measured with closed-path eddy-covariance systems with short sampling lines, Agricultural and Forest Meteorology, 165, 53–63, https://doi.org/10.1016/j.agrformet.2012.05.018, 2012.

Gerardo-Nieto, O., Vega-Peñaranda, A., Gonzalez-Valencia, R., Alfano-Ojeda, Y., and Thalasso, F.: Continuous Measurement of Diffusive and Ebullitive Fluxes of Methane in Aquatic Ecosystems by an Open Dynamic Chamber Method, Environmental Science & Technology, 53, 5159–5167, https://doi.org/10.1021/acs.est.9b00425, 2019.

Guseva, S., Armani, F., Desai, A. R., Dias, N. L., Friborg, T., Iwata, H., Jansen, J., Lükő, G., Mammarella, I., Repina, I., Rutgersson, A., Sachs, T., Scholz, K., Spank, U., Stepanenko, V., Torma, P., Vesala, T., and Lorke, A.: Bulk Transfer Coefficients Estimated From Eddy-Covariance Measurements Over Lakes and Reservoirs, Journal of Geophysical Research: Atmospheres, 128, e2022JD037 219, https://doi.org/10.1029/2022JD037219, 2023.

Juutinen, S., Alm, J., Larmola, T., Huttunen, J. T., Morero, M., Martikainen, P. J., and Silvola, J.: Major implication of the littoral zone for methane release from boreal lakes, Global Biogeochemical Cycles, 17, https://doi.org/10.1029/2003GB002105, 2003.

Kljun, N., Calanca, P., Rotach, M. W., and Schmid, H. P.: A Simple Parameterisation for Flux Footprint Predictions, Boundary-Layer Meteorology, 112, 503–523, https://doi.org/10.1023/B:BOUN.0000030653.71031.96, 2004.

Kremer, J. N., Nixon, S. W., Buckley, B., and Roques, P.: Technical note: Conditions for using the floating chamber method to estimate air-water gas exchange, Estuaries, 26, 985–990, https://doi.org/10.1007/BF02803357, 2003.

Lang, V., Gartiser, V., Hartmann, P., and Maier, M.: Trend analysis of methane uptake in 13 forest soils based on up to 24 years of field measurements in south-west Germany, Agricultural and Forest Meteorology, 375, 110 823, https://doi.org/10.1016/j.agrformet.2025.110823, 2025.

Langelier, W. F.: Effect of Temperature on the pH of Natural Waters, Journal American Water Works Association, 38, 179–185, 1946.

LI-COR Biosciences: Eddy Covariance Processing Software, https://www.licor.com/EddyPro, version 7.0.9, 2021.

Loken, L. C., Crawford, J. T., Schramm, P. J., Stadler, P., Desai, A. R., and Stanley, E. H.: Large Spatial and Temporal Variability of Carbon Dioxide and Methane in a Eutrophic Lake, Journal of Geophysical Research: Biogeosciences, 124, 2248–2266, https://doi.org/10.1029/2019JG005186, 2019.

Lundin, E. J., Giesler, R., Persson, A., Thompson, M. S., and Karlsson, J.: Integrating carbon emissions from lakes and streams in a subarctic catchment, Journal of Geophysical Research: Biogeosciences, 118, 1200–1207, https://doi.org/10.1002/jgrg.20092, 2013.

Malerba, M. E., Edwards, B., Schuster, L., Odebiri, O., Glen, J., Kelly, R., Phan, P., Grinham, A., and Macreadie, P. I.: Technical note: Pondi – a low-cost logger for long-term monitoring of methane, carbon dioxide, and nitrous oxide in aquatic and terrestrial systems, Biogeosciences, 22, 5051–5067, https://doi.org/10.5194/bg-22-5051-2025, 2025.

Martin Bland, J. and Altman, D. G.: Statistical Methods for Assessing Agreement between Two Methods of Clinical Measurement, The Lancet, 327, 307–310, https://doi.org/10.1016/S0140-6736(86)90837-8, 1986.

Martinsen, K. T., Kragh, T., and Sand-Jensen, K.: Technical note: A simple and cost-efficient automated floating chamber for continuous measurements of carbon dioxide gas flux on lakes, Biogeosciences, 15, 5565–5573, https://doi.org/10.5194/bg-15-5565-2018, 2018.

https://doi.org/10.5194/egusphere-2026-2262
Preprint. Discussion started: 26 May 2026

Moncrieff, J. B., Clement, R., Finnigan, J., and Meyers, T.: Averaging, detrending and filtering of eddy covariance time series, in: Handbook of Micrometeorology: A Guide for Surface Flux Measurements, edited by Lee, X., Massman, W. J., and Law, B. E., pp. 7–31, Kluwer Academic, Dordrecht, https://doi.org/10.1007/1-4020-2265-4_2, 2004.

Moran, P. A. P.: Notes on Continuous Stochastic Phenomena, Biometrika, 37, 17–23, http://www.jstor.org/stable/2332142, 1950.

Natchimuthu, S., Sundgren, I., Gålfalk, M., Klemedtsson, L., Crill, P., Danielsson, A., and Bastviken, D.: Spatio-temporal variability of lake CH_4 fluxes and its influence on annual whole lake emission estimates, Limnology and Oceanography, 61, S13–S26, https://doi.org/10.1002/lno.10222, 2016.

Natchimuthu, S., Sundgren, I., Gålfalk, M., Klemedtsson, L., and Bastviken, D.: Spatiotemporal variability of lake pCO_2 and CO_2 fluxes in a hemiboreal catchment, Journal of Geophysical Research: Biogeosciences, 122, 30–49, https://doi.org/10.1002/2016JG003449, 2017.

Oviedo-Vargas, D., Dierick, D., Genereux, D. P., and Oberbauer, S. F.: Chamber measurements of high CO_2 emissions from a rainforest stream receiving old C-rich regional groundwater, Biogeochemistry, 130, 69–83, https://doi.org/10.1007/s10533-016-0243-3, 2016.

Podgrajsek, E., Sahlée, E., Bastviken, D., Holst, J., Lindroth, A., Tranvik, L., and Rutgersson, A.: Comparison of floating chamber and eddy covariance measurements of lake greenhouse gas fluxes, Biogeosciences, 11, 4225–4233, https://doi.org/10.5194/bg-11-4225-2014, 2014.

Pose, S., Reitmann, S., Licht, G. J., Grab, T., and Fieback, T.: AI-Prepared Autonomous Freshwater Monitoring and Sea Ground Detection by an Autonomous Surface Vehicle, Remote Sensing, 15, 860, https://doi.org/10.3390/rs15030860, 2023.

Praetzel, L. S. E., Schmiedeskamp, M., and Knorr, K.-H.: Temperature and sediment properties drive spatiotemporal variability of methane ebullition in a small and shallow temperate lake, Limnology and Oceanography, 66, 2598–2610, https://doi.org/10.1002/lno.11775, 2021.

Rey, S. J. and Anselin, L.: PySAL: A Python Library of Spatial Analytical Methods, pp. 175–193, Springer Berlin Heidelberg, Berlin, Heidelberg, https://doi.org/10.1007/978-3-642-03647-7_11, 2010.

Sabbatini, S., Mammarella, I., Arriga, N., Fratini, G., Graf, A., Hörtnagl, L., Ibrom, A., Longdoz, B., Mauder, M., Merbold, L., Metzger, S., Montagnani, L., Pitacco, A., Rebmann, C., Sedlák, P., Šigut, L., Vitale, D., and Papale, D.: Eddy covariance raw data processing for CO_2 and energy fluxes calculation at ICOS ecosystem stations, International Agrophysics, 32, 495–515, https://doi.org/10.1515/intag-2017-0043, 2018.

Schubert, C. J., Diem, T., and Eugster, W.: Methane Emissions from a Small Wind Shielded Lake Determined by Eddy Covariance, Flux Chambers, Anchored Funnels, and Boundary Model Calculations: A Comparison, Environmental Science & Technology, 46, 4515–4522, https://doi.org/10.1021/es203465x, 2012.

Snyder, L., Potter, J. D., and McDowell, W. H.: An Evaluation of Nitrate, fDOM, and Turbidity Sensors in New Hampshire Streams, Water Resources Research, 54, 2466–2479, https://doi.org/10.1002/2017WR020678, 2018.

Spafford, L. and Risk, D.: Spatiotemporal Variability in Lake-Atmosphere Net CO_2 Exchange in the Littoral Zone of an Oligotrophic Lake, Journal of Geophysical Research: Biogeosciences, 123, 1260–1276, https://doi.org/10.1002/2017JG004115, 2018.

Swedish Meteorological and Hydrological Institute (SMHI): Meteorological data for station Abisko Aut (Station 188790), https://www.smhi.se/data/hitta-data-for-en-plats/ladda-ner-vaderobservationer/, accessed on November 12, 2025, 2025.

Sø, J. S., Sand-Jensen, K., Martinsen, K. T., Polauke, E., Kjær, J. E., Reitzel, K., and Kragh, T.: Methane and carbon dioxide fluxes at high spatiotemporal resolution from a small temperate lake, Science of The Total Environment, 878, 162 895, https://doi.org/10.1016/j.scitotenv.2023.162895, 2023.

Than Duc, N., Silverstein, S., Lundmark, L., Reyier, H., Crill, P., and Bastviken, D.: Automated Flux Chamber for Investigating Gas Flux at Water–Air Interfaces, Environmental Science & Technology, 47, 968–975, https://doi.org/10.1021/es303848x, 2013.

https://doi.org/10.5194/egusphere-2026-2262
Preprint. Discussion started: 26 May 2026

Tian, H., Deng, Y., Liu, Y., Sun, X., Shi, H., Xu, J., Liu, W., Ye, S., Wang, B., Gan, Y., Du, Y., and Wang, Y.: Spatial variability of methane fluxes driven by lacustrine groundwater discharge and its influence on lake methane emissions, Water Research, 285, 124 168, https://doi.org/10.1016/j.watres.2025.124168, 2025.

Uieda, L.: Verde: Processing and gridding spatial data using Green's functions, Journal of Open Source Software, 3, 957, https://doi.org/10.21105/joss.00957, 2018.

Vogt, J., El-Madany, T. S., Héjja, I., Bolek, A., Pratt, E., and Goeckede, M.: BlueMinerva: 3D view, datalogger program, wiring diagram, and mission file example, https://doi.org/10.5281/zenodo.19136563, 2026a.

Vogt, J., El-Madany, T. S., Pratt, E., and Goeckede, M.: Carbon flux, bathymetry and vertical profile data collected with the BlueMinerva at Dagow Lake, Germany, https://doi.org/10.5281/zenodo.19365068, [Data set], 2026b.

Wik, M., Crill, P. M., Varner, R. K., and Bastviken, D.: Multiyear measurements of ebullitive methane flux from three subarctic lakes, Journal of Geophysical Research: Biogeosciences, 118, 1307–1321, https://doi.org/10.1002/jgrg.20103, 2013.

Yin, J., Chen, X., Wen, L., Tu, X., Xie, W., and Xv, R.: Spatial and seasonal variations of carbon emissions in an urban lake: Flux sensitivity and sampling optimization based on high-resolution measurements, Journal of Hydrology, 648, 132 472, https://doi.org/10.1016/j.jhydrol.2024.132472, 2025.

Zug, S., Licht, G., Börner, E., de Souza Mota, E., Monteiro Bezerra de Lima, R., Roeder, E., and Matschullat, J.: Taking the pulse of nature – how robotics and sensors assist in lake and reservoir management, Geoscientific Instrumentation, Methods and Data Systems, 14, 167–181, https://doi.org/10.5194/gi-14-167-2025, 2025.

Zwillinger, D. and Kokoska, S.: CRC Standard Probability and Statistics Tables and Formulae, Chapman & Hall, New York, 2000.